ORGANIC LETTERS

2010
Vol. 12, No. 21
5000−5003

Ambipolar Hexa-*peri*-hexabenzocoronene−Fullerene Hybrid Materials

Wallace W. H. Wong,*,† Doojin Vak,† Th. Birendra Singh,‡ Shijie Ren,† Chao Yan,† David J. Jones,† Irving I. Liaw,† Robert N. Lamb,† and Andrew B. Holmes†

School of Chemistry, University of Melbourne, Victoria 3010, Australia, and CSIRO Molecular and Health Technologies, Ian Wark Laboratory, Clayton South, Victoria 3169, Australia

wwhwong@unimelb.edu.au

Received September 10, 2010

ABSTRACT

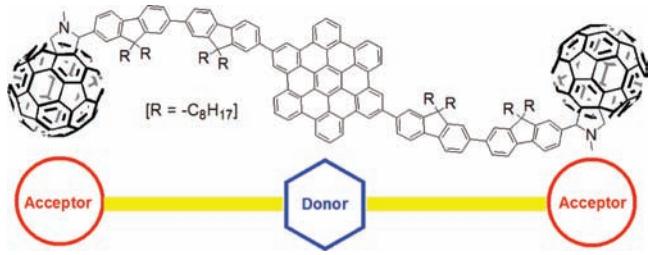

A new class of self-assembling hexa-*peri*-hexbenzocoronene (HBC)−fullerene hybrid materials has been synthesized and characterized. Photoluminescence experiments indicate that energy transfer processes can be tuned in these donor−acceptor systems by varying the length and nature of the linker group. In preliminary device testing, ambipolar charge transport behavior is observed in organic field effect transistors, while single active component organic photovoltaic devices consisting of these materials achieved a maximum external quantum efficiency of 30%.

The arrangement of electron donor (D) and electron acceptor (A) materials in heterojunction organic photovoltaic (OPV) devices is a determining factor in device performance. One approach is to use block copolymers to achieve nanoscale morphology. In these systems, D and A blocks are covalently linked and the blocks phase separate according to the size of the D and A blocks. Several groups have demonstrated this concept,[1−3] and the benchmark for the power conversion efficiency of these OPV devices is at 1.7%.[4] Small molecule or oligomeric D−A materials are also potential candidates in single component OPV devices. Several examples of donor−acceptor dyad molecules have been tested in OPV devices.[5−11] The best oligomeric system, with efficiency up to 1.5%, showed assembly of nanoscale D−A morphology containing highly ordered domains.[12,13]

† University of Melbourne.
‡ CSIRO Molecular and Health Technologies.

(1) Sommer, M.; Huttner, S.; Steiner, U.; Thelakkat, M. *Appl. Phys. Lett.* **2009**, *95*, DOI:, 10.1063/1.3257367.
(2) Zhang, Q. L.; Cirpan, A.; Russell, T. P.; Emrick, T. *Macromolecules* **2009**, *42*, 1079.
(3) Dante, M.; Yang, C.; Walker, B.; Wudl, F.; Nguyen, T. Q. *Adv. Mater.* **2010**, *22*, 1835.
(4) Miyanishi, S.; Zhang, Y.; Tajima, K.; Hashimoto, K. *Chem. Commun.* **2010**, *46*, 6723.
(5) Maggini, M.; Possamai, G.; Menna, E.; Scorrano, G.; Camaioni, N.; Ridolfi, G.; Casalbore-Miceli, G.; Franco, L.; Ruzzi, M.; Corvaja, C. *Chem. Commun.* **2002**, *2028*.
(6) Possamai, G.; Maggini, M.; Menna, E.; Scorrano, G.; Franco, L.; Ruzzi, M.; Corvaja, C.; Ridolfi, G.; Samori, P.; Geri, A.; Camaioni, N. *Appl. Phys. A: Mater. Sci. Process.* **2004**, *79*, 51.
(7) Nierengarten, J. F. *Sol. Energy Mater. Sol. Cells* **2004**, *83*, 187.
(8) Nierengarten, J. F.; Gu, T.; Aernouts, T.; Geens, W.; Poortmans, J.; Hadziioannou, G.; Tsamouras, D. *Appl. Phys. A: Mater. Sci. Process.* **2004**, *79*, 47.
(9) Meng, F. S.; Hua, J. L.; Chen, K. C.; Tian, H.; Zuppiroli, L.; Nuesch, F. *J. Mater. Chem.* **2005**, *15*, 979.
(10) Negishi, N.; Yamada, K.; Takimiya, K.; Aso, Y.; Otsubo, T.; Harima, Y. *Chem. Lett.* **2003**, *32*, 404.
(11) Yamamoto, Y.; Zhang, G. X.; Jin, W. S.; Fukushima, T.; Ishii, N.; Saeki, A.; Seki, S.; Tagawa, S.; Minari, T.; Tsukagoshi, K.; Aida, T. *Proc. Natl. Acad. Sci. U.S.A.* **2009**, *106*, 21051.
(12) Bu, L. J.; Guo, X. Y.; Yu, B.; Qu, Y.; Xie, Z. Y.; Yan, D. H.; Geng, Y. H.; Wang, F. S. *J. Am. Chem. Soc.* **2009**, *131*, 13242.
(13) Nishizawa, T.; Lim, H. K.; Tajima, K.; Hashimoto, K. *Chem. Commun.* **2009**, *2469*.

10.1021/ol102166m
Published on Web 10/04/2010

Scheme 1. Synthesis of Fullerene−Hexa-*peri*-hexabenzocoronene−Fullerene Triads **1** and **2**

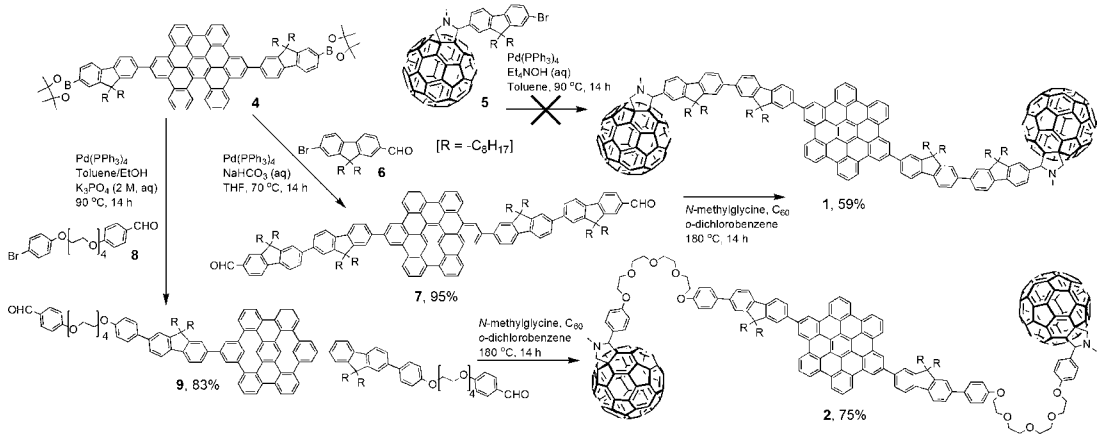

Scheme 2. Synthesis of Hexa-*peri*-hexabenzocoronene−Fullerene Dyad **3**

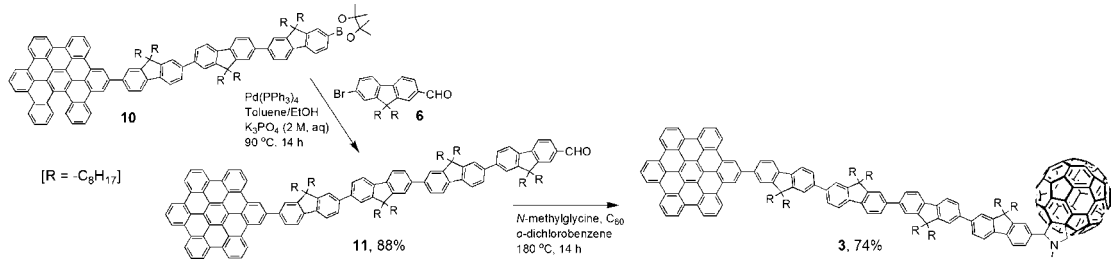

Hexa-*peri*-hexabenzocoronene (HBC) is a planar aromatic molecule and has been shown to self-assemble into columnar[14−17] and nanotube[11,18] structures in solution and in solid state. Recently, we reported the synthesis and optoelectronic properties of a highly soluble functional HBC building block carrying conjugated substituents.[19−21] The 9,9-dioctylfluorenyl hexa-*peri*-hexabenzocoronene (FHBC) moiety has emerged as a material with excellent solubility and the potential for further derivatization. In this study, we report the synthesis, characterization, and device properties of a series of FHBC−fullerene D−A materials. By taking advantage of the self-assembling properties of the FHBC core, there is potential to achieve an ordered D−A morphology that is beneficial for OPV device performance.

The strategy for the synthesis of the ambipolar hexa-*peri*-hexabenzocoronene−fullerene materials is based on the highly soluble FHBC core unit. In all cases, the fullerene moieties are connected to the FHBC derivatives in the last step of the synthesis sequence through the well-known 1,3-dipolar cycloaddition of azomethine ylids to the fullerene (Schemes 1 and 2). One interesting observation is that initial attempts to connect the FHBC boronic acid pinacol ester derivative **4** and fullerene derivative **5** using palladium-catalyzed carbon−carbon bond formation proved unsuccessful (Scheme 1). Very few examples of palladium-catalyzed coupling involving fullerene derivatives can be found in the literature.[22−28] The experimental observations in this study suggest the fullerene derivatives are easily reduced by palladium(0) species. This redox reaction probably

(14) Wu, J.; Pisula, W.; Müllen, K. *Chem. Rev.* **2007**, *107*, 718.
(15) Herwig, P.; Kayser, C. W.; Müllen, K.; Spiess, H. W. *Adv. Mater.* **1996**, *8*, 510.
(16) Ito, S.; Wehmeier, M.; Brand, J. D.; Kubel, C.; Epsch, R.; Rabe, J. P.; Müllen, K. *Chem.−Eur. J.* **2000**, *6*, 4327.
(17) Kastler, M.; Pisula, W.; Wasserfallen, D.; Pakula, T.; Müllen, K. *J. Am. Chem. Soc.* **2005**, *127*, 4286.
(18) Hill, J. P.; Jin, W.; Kosaka, A.; Fukushima, T.; Ichihara, H.; Shimomura, T.; Ito, K.; Hashizume, T.; Ishii, N.; Aida, T. *Science* **2004**, *304*, 1481.
(19) Wong, W. W. H.; Jones, D. J.; Yan, C.; Watkins, S. E.; King, S.; Haque, S. A.; Wen, X.; Ghiggino, K. P.; Holmes, A. B. *Org. Lett.* **2009**, *11*, 975.
(20) Wong, W. W. H.; Ma, C.-Q.; Pisula, W.; Yan, C.; Feng, X. L.; Jones, D. J.; Müllen, K.; Janssen, R. A.; Bäuerle, P.; Holmes, A. B. *Chem. Mater.* **2010**, *22*, 457.
(21) Wong, W. W. H.; Singh, T. B.; Vak, D.; Pisula, W.; Yan, C.; Feng, X. L.; Williams, E. L.; Chan, K. L.; Mao, Q.; Jones, D. J.; Ma, C.-Q.; Müllen, K.; Bäuerle, P.; Holmes, A. B. *Adv. Funct. Mater.* **2010**, *20*, 927.
(22) Xu, G. D.; Han, Y.; Sun, M. G.; Bo, Z. S.; Chen, C. H. *J. Polym. Sci., Part A: Polym. Chem.* **2007**, *45*, 4696.
(23) Gomez-Escalonilla, M. J.; Langa, F. *Tetrahedron Lett.* **2008**, *49*, 3656.
(24) Katterle, M.; Holzwarth, A. R.; Jesorka, A. *Eur. J. Org. Chem.* **2006**, *414*.
(25) Pierrat, P.; Vanderheiden, S.; Muller, T.; Brase, S. *Chem. Commun.* **2009**, *1748*.
(26) Mori, S.; Nambo, M.; Chi, L.-C.; Bouffard, J.; Itami, K. *Org. Lett.* **2008**, *10*, 4609.
(27) Nambo, M.; Wakamiya, A.; Yamaguchi, S.; Itami, K. *J. Am. Chem. Soc.* **2009**, *131*, 15112.
(28) Filippone, S.; Maroto, E. E.; Martin-Domenech, A.; Suarez, M.; Martin, N. *Nat. Chem.* **2009**, *1*, 578.

Table 1. Thermal, Optical, and Redox Data of the FHBC−Fullerene Compounds

compounds	T_{deg} (°C)[a]	T_g (°C)[b]	λ_{abs}^{max} (nm) solution[c]	λ_{abs}^{max} (nm) film	E_{ox}^{onset} (V)[d]	HOMO (eV)[e]	E_{red}^{onset} (V)[d]	LUMO (eV)[f]	E_g (eV)[g]
1	385	129	370 (2.7) 420 (0.9	372	0.67	−5.47 (−5.41)	−1.00	−3.80	1.67
2	359	125	370 (2.2) 419 (0.6)	372	0.51	−5.31 (−5.39)	−1.00	−3.80	1.51
3	406	127	365 (2.6)	372	0.54	−5.34 (−5.38)	−1.06	−3.74	1.60

[a] Degradation temperature (T_{deg}) observed from TGA corresponding to 5% weight loss at 10 °C/min under nitrogen flow. [b] Glass transition temperature (T_g) from DSC at 10 °C/min under nitrogen flow. [c] Measured in *o*-dichlorobenzene solution and extinction coefficient ($\times 10^5$ M^{-1} cm^{-1}) in brackets. [d] Cyclic voltammograms measured in *o*-dichlorobenzene, 1×10^{-3} M, Bu_4NPF_6 (0.1 M), 295 K, scan rate = 100 mV s^{-1}, versus Fc/Fc^+. [e] Determined from $E_{HOMO} = -(E_{ox}^{onset} + 4.80)$ (eV), data in brackets measured by photoelectron spectroscopy in air.[29,30] [f] Determined from $E_{LUMO} = -(E_{red}^{onset} + 4.80)$ (eV). [g] Energy gap (E_g) = LUMO − HOMO.

maintains the Pd species in the Pd(II) state, and consequently, the Pd catalyst is deactivated. Further studies will be required to ascertain the mechanism of this catalyst deactivation.

The synthesis of FHBC−fullerene hybrids **1** was achieved by first coupling the FHBC boronic acid pinacol ester derivative **4** with 7-bromofluorene-2-carboxaldehyde **6** (Scheme 1). Condensation of aldehydes **7** with *N*- methylglycine gave the azomethine ylid intermediate which reacted with C_{60} to give FHBC−fullerene hybrid **1**. The FHBC−fullerene derivative **2**, with a flexible tetraethylene glycol linker between the FHBC and fullerene moieties, was similarly obtained (Scheme 1). Starting from the monosubstituted FHBC boronic acid pinacol ester derivative **10**, FHBC−fullerene dyad **3** was obtained in good yield after coupling with aldehyde **6** followed by 1,3-dipolar cycloaddition to C_{60} (Scheme 2). Typically, an excess of C_{60} was added to the 1,3-dipolar cycloaddition reactions in order to drive the reaction to completion. The relatively low molecular weight C_{60} can be easily separated from the desired products by size exclusion chromatography. The identity and purity of all new compounds were verified by a range of standard analytical techniques (see Supporting Information).

All three FHBC−fullerene hybrid materials **1**, **2**, and **3** showed good thermal stability in thermal gravimetric analysis (TGA) experiments (Table 1). In differential scanning calorimetry (DSC) experiments, a weak transition at around 125 °C was observed for the three compounds and can be assigned to the rearrangement of the alkyl side chains on the fluorene moieties (Table 1). All three FHBC−fullerene compounds have their absorption maximum at ~370 nm and can be assigned to the absorption band of the FHBC unit (Figure 1). The solution PL spectra of the compounds (10^{-4} M in *o*-dichlorobenzene) were recorded using 370 nm excitation (Figure 1). The relative PL intensities observed are in agreement with the different spatial separation between the donor FHBC and acceptor fullerene units in compounds **1**, **2**, and **3**. For compound **1**, two fullerene units are separated from the HBC core by two fluorene units and showed very weak fluorescence from the HBC unit. On the other hand, compound **2** has a tetra(ethylene glycol) linker between the HBC and the fullerene, while compound **3** has a four-fluorene spacer. In these cases, the emission from the HBC unit is relatively strong compared with that of compound **1** at the same solution concentration. Time-resolved

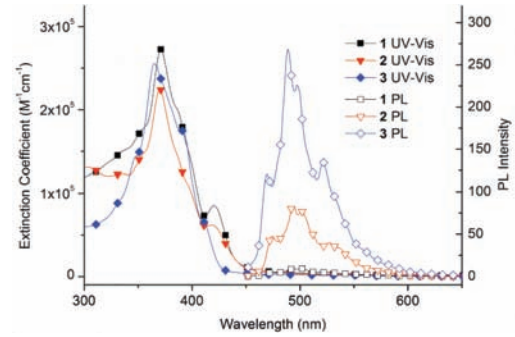

Figure 1. UV−vis absorption and photoluminescence (PL) spectra of FHBC−fullerene compounds in *o*-dichlorobenzene solution.

spectroscopic experiments are now in progress to determine the energy transfer mechanisms involved. Photoluminescence was not observed in solid state samples of the compounds (films with 50 nm thickness). This indicates close packing of the FHBC−fullerene molecules in the solid state with quenching of the FHBC fluorescence by the fullerene moieties. In electrochemical experiments, the FHBC−fullerene compounds showed reversible reductions typical of fullerene derivatives (Table 1). The oxidation of these materials closely matches that of the parent FHBC compound (see Supporting Information for cyclic voltammograms).

From previous studies, it is well-known that the FHBC moiety aggregates strongly in solution and assembles into ordered structures in the solid state.[20,21] Similar behavior was also observed for the ambipolar FHBC−fullerene hybrid materials. In solution NMR spectroscopic studies, the resonances assigned to the FHBC protons shift significantly upfield with increasing concentration of the hybrid materials. Figure 2 shows the concentration-dependent ^{1}H NMR spectrum of compound **3** (see Supporting Information for ^{1}H NMR spectrum of **1** and **2**). Protons on the periphery of cyclic aromatic systems usually appear downfield because of the ring current effect. The upfield shift of the FHBC

(29) Kane, E. O. *Phys. Rev.* **1962**, *127*, 131.
(30) Kirihata, H.; Uda, M. *Rev. Sci. Instrum.* **1981**, *52*, 68.

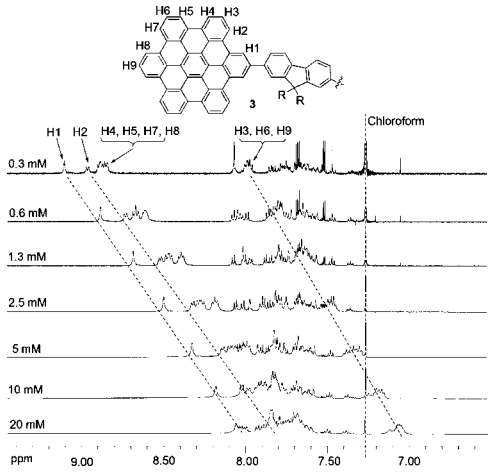

Figure 2. ^{1}H NMR spectrum of FHBC−fullerene dyad **3** at various concentrations in $CDCl_3$.

proton resonances with increasing concentration is indicative of $\pi-\pi$ stacking of the FHBC core. Interestingly, there is little change in the resonances belonging to protons of the fluorene and fullerene units on these hybrid compounds. This suggests a strong $\pi-\pi$ interaction of the FHBC cores with the peripheral fullerene units arranged in a staggered manner. The solid-state structure of the FHBC−fullerene compounds were examined using X-ray diffraction experiments. Films of the compounds were deposited onto ultrathin silicon substrate, and two-dimensional X-ray scattering patterns were recorded (see Supporting Information). The two-dimensional wide-angle X-ray scattering (2D-WAXS) was carried out at SAXS/WAXS beamline in the Australian Synchrotron with wavenumber of 0.62A. The scattering patterns revealed that the $\pi-\pi$ stacking distances for compounds **1**, **2**, and **3** are 0.351, 0.358, and 0.341 nm, respectively. This is consistent with our previous reports on FHBC materials.[21] The minor variations in $\pi-\pi$ stacking distance is probably a result of the steric hindrance of the different fullerene substituents in the three compounds.

The charge transport properties of the FHBC−fullerene hybrid compounds were examined by incorporating these materials into organic field effect transistors (OFET). Bottom gate bottom contact OFETs were fabricated by depositing the organic semiconductor from *o*-dichlorobenzene solution by spin coating onto a lithographically patterned substrate (see Supporting Information for details). A summary of charge mobility values for the OFET devices is presented in Table 2 (see Supporting Information for current−voltage data). It is clear that the OFET devices show ambipolar behavior with reasonable hole (μ_{hole}) and electron ($\mu_{electron}$) mobilities that are comparable to those of a HBC−fullerene system previous reported.[11] More importantly, the hole and electron mobilities in each of the devices containing compounds **1**, **2**, and **3** are well balanced.

Given such encouraging OFET data, a preliminary attempt was made to use these ambipolar materials as the single active component in heterojunction organic photovoltaic (OPV) devices. OPV devices with the structure ITO|PEDOT:PSS|active layer|TiO_x/Al [ITO, indium tin oxide; PEDOT:PSS, poly(3,4-ethylenedioxythiophene):poly(styrenesulfonate)] were fabricated and characterized. The active layer of FHBC−fullerene hybrid material was deposited from *o*-dichlorobenzene solution by spin coating giving films of ∼50 nm. TiOx layers were introduced by following literature procedures.[31] In general, all devices showed good diode-like behavior in the dark and photovoltaic effects under simulated AM 1.5 G illumination. Table 2 summarizes the device performance of the various solar cells, and the following characteristic parameters are given: short-circuit currents (J_{sc}), open-circuit voltages (V_{oc}), fill factors (*FF*), and power conversion efficiencies (η). The current density to voltage curves and external quantum efficiency (EQE) spectra of selected devices can be found in Supporting Information. Although the power conversion efficiencies of these devices are rather modest, a maximum EQE of 30% was recorded for the device containing compound **3** at 390 nm. This value is an order of magitude higher than that reported for a previous HBC−fullerene system.[11] Given the thickness of the active layers (∼50 nm) and the short wavelength absorption of these materials, there is potential for improvement in this class of materials. One of the major loss mechanisms in efficiency is thought to be charge recombination, particularly for FHBC−fullerene derivative **1**. Time-resolved spectroscopic studies are currently underway to ascertain the rates of charge separation and recombination in these systems. In addition, our group is actively pursuing further structural variations in these FHBC−fullerene systems in order to improve spectral absorption as well as solid state D−A morphology.

Table 2. OFET and OPV Device Performance

	OFET		OPV[a]			
	μ_{hole}, $cm^2/(Vs)$	$\mu_{electron}$, $cm^2/(Vs)$	J_{sc}, mA/cm^2	V_{oc}, V	*FF*	η, %
1	2.1×10^{-7}	4.7×10^{-7}	0.80	0.90	0.21	0.15
2	4.4×10^{-7}	0.7×10^{-7}	0.37	0.78	0.22	0.06
3	3.4×10^{-6}	2.0×10^{-6}	0.87	0.80	0.31	0.22

[a] The data shown are average values over several devices.

Acknowledgment. We thank the Australian Research Council (ARC) for Discovery Projects (DP0451189, DP0877325), the Victorian Government (DPI−VICOSC), the Commonwealth Scientific and Industrial Research Organisation (CSIRO), and the University of Melbourne for generous financial support. The X-ray experiments were undertaken on the SAXS/WAXS beamline at the Australian Synchrotron, Victoria, Australia.

Supporting Information Available: Experimental procedures, full spectroscopic data for all new compounds, and device data. This material is available free of charge via the Internet at http://pubs.acs.org.

OL102166M

(31) Park, S. H.; Roy, A.; Beaupré, S.; Cho, S.; Coates, N. E.; Moon, J. S.; Moses, D.; Leclerc, M.; Lee, K.; Heeger, A. J. *Nat. Photon.* **2009**, *3*, 297.